Theoretical investigation of the Fermi surfaces of $La_{2-x}Sr_xCuO_4$ and $YBa_2Cu_3O_7$

V. N. Antonov, Vl. N. Antonov, V. G. Bar'yakhtar, A. I. Baglyuk, E. G. Maksimov,
V. V. Nemoshkalenko, A. Ya. Perlov, S. Yu. Savrasov, and Yu. A. Uspenskii

Institute of Metal Physics, Academy of Sciences of the Ukrainian SSR, Kiev

A theoretical investigation is made of the shape of the Fermi surface and of the constant-energy surfaces near the Fermi energy of the $La_{2-x}Sr_xCuO_4$ and $YBa_2Cu_3O_7$ oxides by a self-consistent linear muffin-tin orbital method in the atomic sphere approximation (LMTO-ASA). It is shown that the Fermi surfaces of these compounds are strongly two-dimensional. The Fermi surface of $La_{2-x}Sr_xCuO_4$ is a corrugated rounded box centered at the point Γ. The Fermi surface of $YBa_2Cu_3O_7$ consists of four sheets: an electron "cushion" at the point Γ and three nested hole surfaces centered at the point S. The electron cushion and one of the hole surfaces are strongly corrugated along the z direction. The theoretically calculated Fermi surfaces of La_2CuO_4 and $YBa_2Cu_3O_7$ are compared with the experimental data on electron–positron annihilation. Maps of electron velocities are given and the results are reported of numerical calculations of various characteristics such as the sheet areas, mean velocities, mean-square velocities, and partial densities of states for each sheet of the Fermi surface of $YBa_2Cu_3O_7$.

Much work has been done on the electron structure of the high-temperature superconductors La–Sr–Cu–O and Y–Ba–Cu–O since their discovery.[1,2] The energy structure of the valence band of high-temperature superconductors has now been accurately established both by band calculations and by various spectroscopic experimental methods. However, much less attention has been given to the Fermi surfaces of these substances. This has been due to objective difficulties. In view of the high temperature of the transition to the superconducting state, the usual experimental meth-

ods for the investigation of the Fermi surfaces based on magnetic oscillations are inapplicable to high-temperature superconductors. In practice, the only method that can be used to study the structure of the Fermi surfaces of high-temperature superconductors is that of electron–positron annihilation. There is only one published paper reporting a study of the Fourier distribution of the electron density and a qualitative construction of the Fermi surfaces of La_2CuO_4 and $La_{1.82}Sr_{0.18}CuO_4$ by the electron–positron annihilation method.[3] Experimental studies of the Fermi surface of $YBaCu_3O_{7-\delta}$ are reported in Refs. 4–6. As a result of the very first calculations of the energy band structure of high-temperature superconductors,[7–9] theoretical studies of the Fermi surfaces have yielded the sections of the Fermi surface, but only in the symmetric $k_z = 0$ plane. Moreover, the number of points k at which these calculations have been carried out is very limited. Consequently, all the results reported in Refs. 7–9 should be regarded as only qualitative. Detailed investigations of the Fermi surfaces of high-tem-
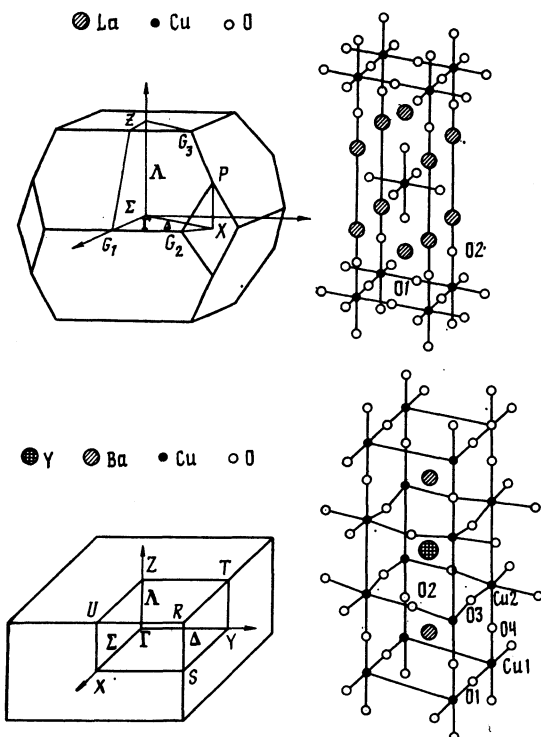
FIG. 1. Crystal structures and Brillouin zones of La_2CuO_4 and $YBa_2Cu_3O_7$.
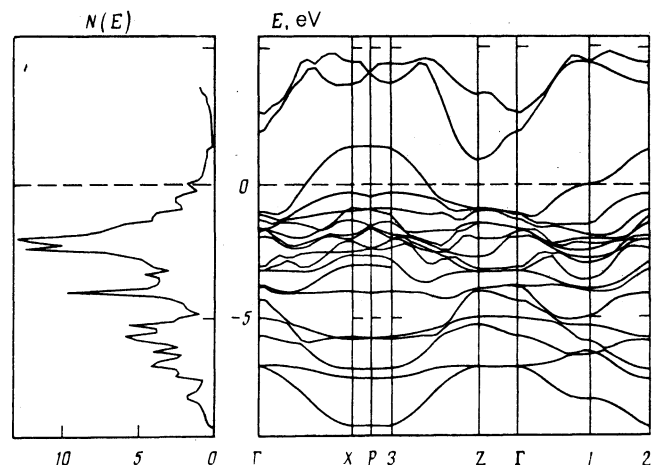
FIG. 2. Band structure and the total density of states $N(E)$ (electrons per electron volt per cell) in La_2Cu_4.
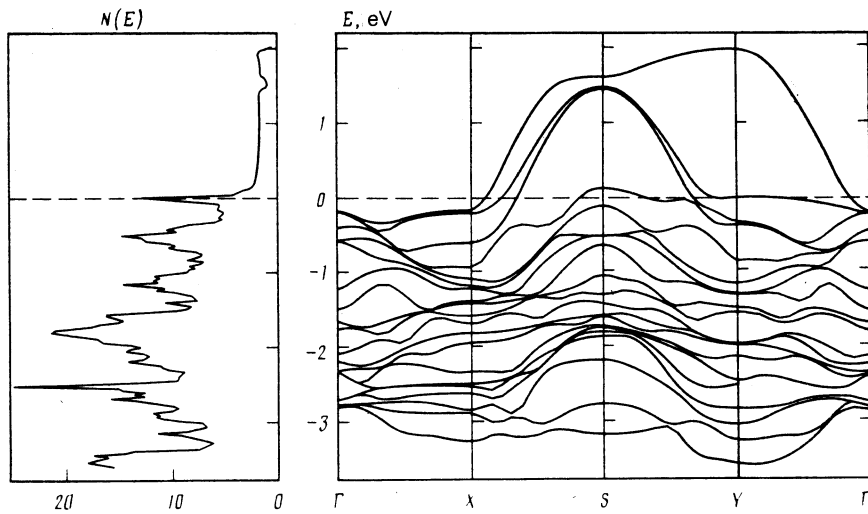
FIG. 3. Band structure and the total density of states $N(E)$ (electrons per electron volt per cell) in $YBa_2Cu_3O_7$.

perature superconductors are an important task, because it should help in identifying the nature of superconductivity in these substances. Our aim will be to carry out a theoretical investigation of the shape of the Fermi surface and of constant-energy surfaces near the Fermi energy of $La_{2-x}Sr_x CuO_4$ and $YBa_2Cu_3O_7$.

The energy band structure of the high-temperature superconductors La_2CuO_4 and $YBa_2Cu_3O_7$ was calculated by a self-consistent linear muffin-tin orbital method in the atomic sphere approximation (LMTO-ASA).[10] The calculations were carried out allowing for all the relativistic corrections, with the exception of the spin–orbit interaction, which in the case of these two compounds is small compared with the width of the valence band. The exchange-correlation potential was based on a local approximation in the theory of the electron density functional.[11]

The self-consistent calculation of the energy band structure of La_2CuO_4 was carried out at 57 points in the irreducible part of the Brillouin zone (BZ). In the process of ensuring self-consistency we considered all the atomic electrons (unfrozen core approximation). The wave function expansions included all the terms up to $l = 3$ for La and Cu

and up to $l = 2$ for oxygen. In the case of $YBa_2Cu_3O_7$, we ensured self-consistency at 39 points in the irreducible part of the BZ. In the wave function expansion of this compound we included terms up to $l = 2$ for yttrium and barium and up to $l = 1$ for oxygen.

Figure 1 shows the crystal structures and the corresponding Brillouin zones, whereas Figs. 2 and 3 give the dispersion curves $E(\mathbf{k})$ and the total densities of states in La_2CuO_4 and $YBa_2Cu_3O_7$. The shape of the dispersion curves agrees quite well with the results published earlier.[7-9]

The Fermi surfaces of these compounds were calculated by the tetrahedron method using the self-consistent poten-
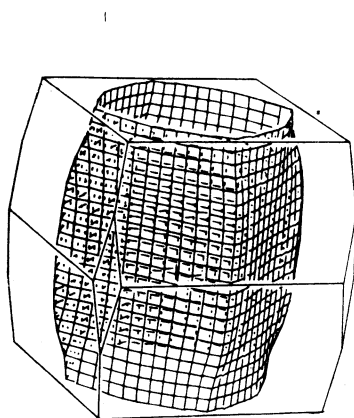
FIG. 4. Fermi surface of La_2CuO_4.
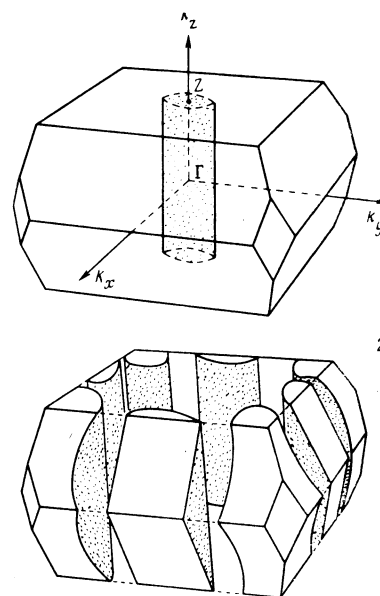
FIG. 5. Fermi surface of $La_{1.82}Sr_{0.18}CuO_4$ reconstructed from the experimental data obtained by the electron–positron annihilation method[3]: 1) electron Fermi surface; 2) hole Fermi surface.

ΔE = 0.0 Ry   0.02

0.04   0.06
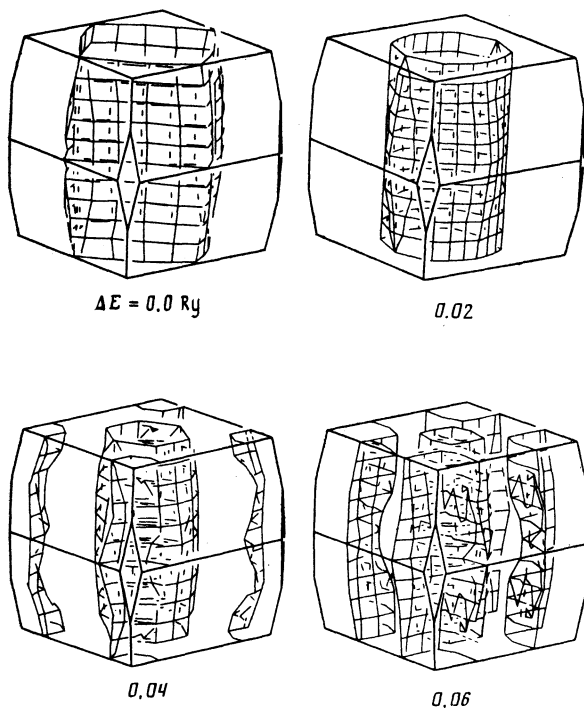
FIG. 6. Constant-energy surfaces representing $E_F - \Delta E$ in the case of La_2CuO_4.

tial obtained as above.[12] At this stage the calculation of $E(k)$ was carried out for a much larger number of points. In the case of La_2CuO_4 we used 595 values of k in $\frac{1}{16}$th part of the BZ, whereas in the case of $YBa_2Cu_3O_7$ we employed 1600 values of k in $\frac{1}{8}$th part of the BZ. It should be pointed out that refinement of these calculations increased almost two-fold the density of states at the Fermi level in the case of $YBa_2Cu_3O_7$. This was due to a more accurate description of the behavior of the band emerging at the Fermi level (along the Γ–Y direction in Fig. 3).

The calculated Fermi surface of La_2CuO_4 is essentially two-dimensional and represents a corrugated box with rounded corners centered on the point Γ and directed along the z axis (Fig. 4). This surface has extended flat regions. A section of the Fermi surface by a plane perpendicular to the z

axis is a rounded square. A section passing through the symmetric point Z is rotated by 45° relative to a section passing through the point Γ. In our opinion this is an important factor because such a corrugation of the Fermi surface prevents perfect "nesting" (with the vector $\mathbf{q}\|\Gamma X$ and $|\mathbf{q}| = 2k_F$) and a structural transition to the orthorhombic phase, which has semiconducting properties.

The results of theoretical calculations are in qualitative agreement with the experimental data obtained in Ref. 3 (Fig. 5). The only difference is the absence of hole cylinders centered at the points X and G_1. However, the agreement with the experimental results improves considerably if we lower the Fermi energy. This should occur if La_2CuO_4 is doped with strontium atoms, i.e., if trivalent lanthanum atoms are replaced with divalent strontium. Figure 6 shows the theoretically calculated constant-energy surfaces representing $E = E_F - \Delta E$ for La_2CuO_4. If we assume that in this case we can use the rigid band approximation, then $\Delta E = 0.02$ Ry corresponds to $La_{1.6}Sr_{0.4}CuO_4$, $\Delta E = 0.04$ Ry corresponds to $La_{1.2}Sr_{0.8}CuO_4$, and $\Delta E = 0.06$ Ry corresponds to $La_{0.5}Sr_{1.5}CuO_4$. Clearly, the rigid band approximation can hardly be valid in such a wide energy range. Nevertheless, even for La_2CuO_4 the constant-energy surface is in qualitative agreement with the experimentally determined Fermi surface.[3]

Figure 7 shows the general shape of the theoretically calculated Fermi surface of YBa_2CuO_7. It is much more complex than the Fermi surface of La_2CuO_4, but again is of quasi-two-dimensional nature. The crystal structure of La_2CuO_4 is characterized by the presence of $Cu–O_1$ planes, whereas in the case of $YBa_2Cu_3O_7$, in addition to the $Cu_2–O_2–O_3$ planes, there are also $Cu_1–O_1$ atomic chains (Fig. 1). The presence of these atomic chains is responsible for the characteristic electron surface centered at the point Γ and shaped like a cushion (Fig. 8). Other parts of the Fermi surface are corrugated nested boxes centered at the point S containing a hole surface in the form of a four-pointed star in the extended zone scheme. Two nesting boxes are also due to holes. The inner box is weakly corrugated along the z axis, whereas the outer box changes considerably as we move along the z axis. This is demonstrated clearly in Fig. 9, which shows the Fermi surface sections for different values of k_z. For $k_z = 0.5\pi/c$, we have a box, whereas for $k_z \approx 0.23\pi/c$
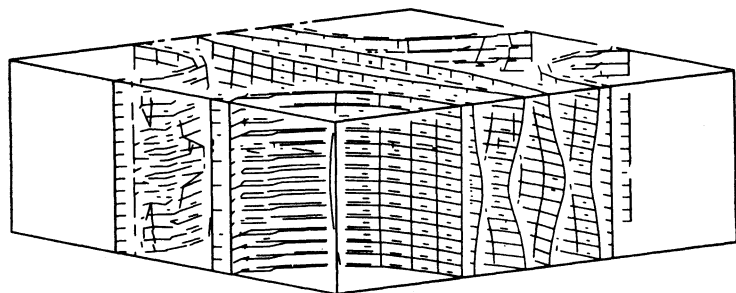
FIG. 7. Fermi surface of $YBa_2Cu_3O_7$ (without hole pockets at the point S).

ке S)
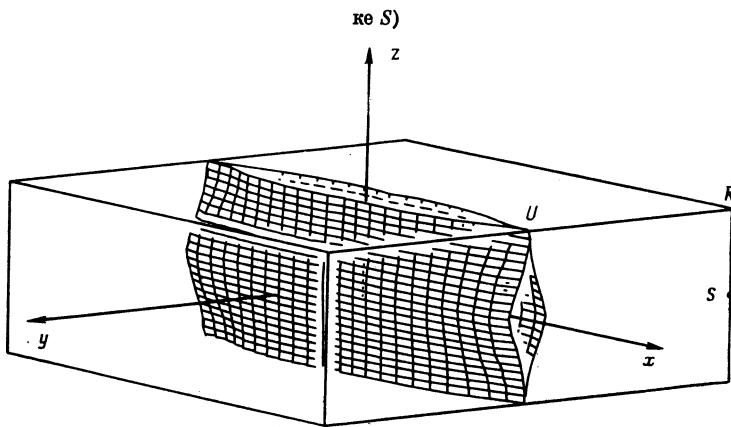
FIG. 8. Electron cushion of the Fermi surface of $YBa_2Cu_3O_7$.

the walls of the box centered at the points S merge, which alters the topology of the Fermi surface sections. Moreover, the central electron cushion is also strongly corrugated. In the $k_z = 0$ plane we have practically parallel lines whereas for $k_z = 0.5\pi/c$ these lines join at the points U.

It is interesting to compare the theoretically calculated Fermi surface of $YBa_2Cu_3O_7$ with that found experimentally by the electron–positron annihilation method. Figure 10a shows different sheets of the Fermi surface of $YBa_2Cu_3O_7$ reconstructed on the basis of the experimental data of Ref. 4. Unfortunately, the spectrometer resolution used in that study was insufficient to determine details for the Fermi surface. Therefore, Fig. 10c shows the Fermi surface reconstructed by the authors of Ref. 4 allowing for the resolution function of the spectrometer and using the results of a calculation reported in Ref. 9. Figure 11 shows the results obtained in the present study. The agreement between the theo-

retically calculated and experimentally determined Fermi surfaces is quite good for all the sheets with the exception of the electron cushion (Fig. 8). This discrepancy is due to the presence of twinning planes in a single crystal of $YBa_2Cu_3O_{7-\delta}$ (Ref. 4). Therefore, the experimental results apply to a quasitetragonal structure, when x and y are equivalent directions.
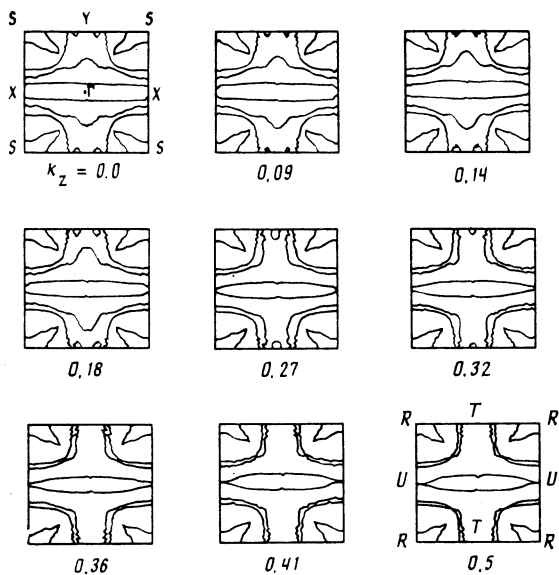
FIG. 9. Sections through the Fermi surface of $YBa_2Cu_3O_7$ formed by k_z = const planes (in units of π/c).
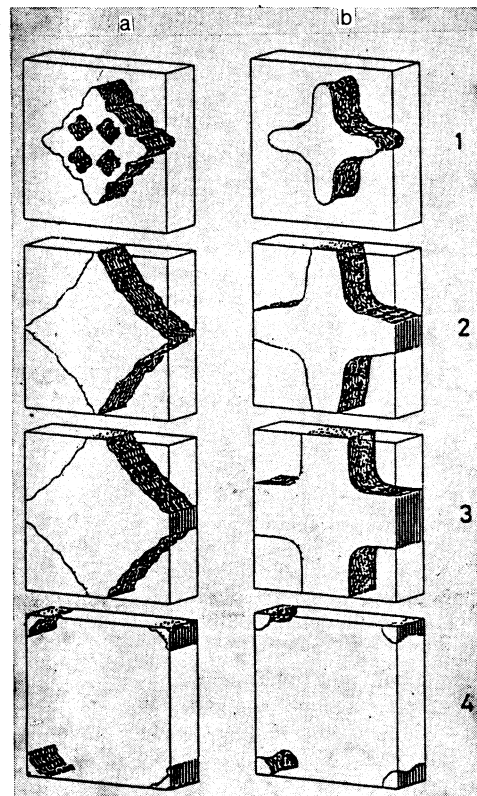
FIG. 10. Fermi surface of $YBa_2Cu_3O_{7-\delta}$ (Ref. 4): a) experimental data obtained by the electron–positron annihilation method; b) reconstruction of the Fermi surface allowing for the experimental resolution function and the results of a calculation reported in Ref. 9.
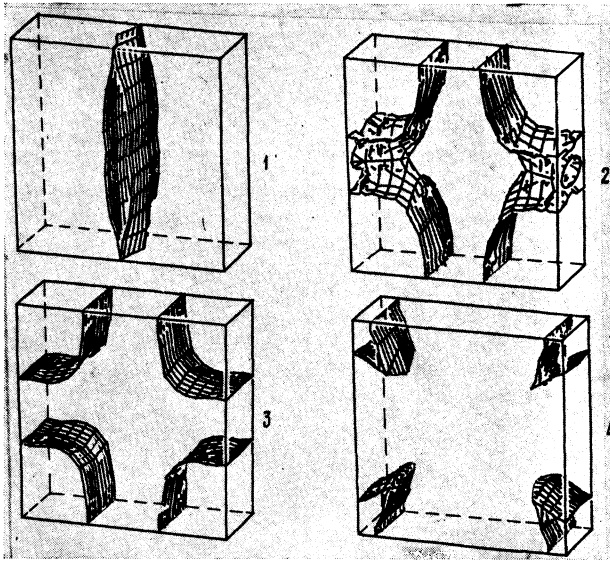
FIG. 11. Theoretically calculated sheets of the Fermi surface of YBa$_2$Cu$_3$O$_7$.

FIG. 13. Distribution of the velocities $V_k(E_F)$ in YBa$_2$Cu$_3$O$_7$ plotted for the $k_z = \pi/s$ section.

In this case, instead of an electron cushion elongated along the x axis, the experiments yield a superposition of two such Fermi sheets along x and y. It should also be pointed out that small hole "pockets" centered at the point S (labeled 4 in Fig. 11) differ slightly in size from the pockets found experimentally in Ref. 4 (labeled 4 in Fig. 10a). This is due to the fact that the theoretical calculations were carried out for the compound YBa$_2$Cu$_3$O$_{7-\delta}$ with $\delta = 0$, whereas in reality we always have $\delta > 0$. In order to allow for the oxygen deficit, we must increase the Fermi energy and since the sheet in question is due to holes, an increase in the Fermi energy reduces its size in exact agreement with the experimental results. In our opinion, a more important circumstance is the strong corrugation of the box outside the point S (labeled 2 in Figs. 9 and 11). However, such fine details of the Fermi surface cannot yet be established reliably at the attainable spectrometer resolution (a large unit cell in the direct space leads to a small BZ, so that the relative resolution is low).
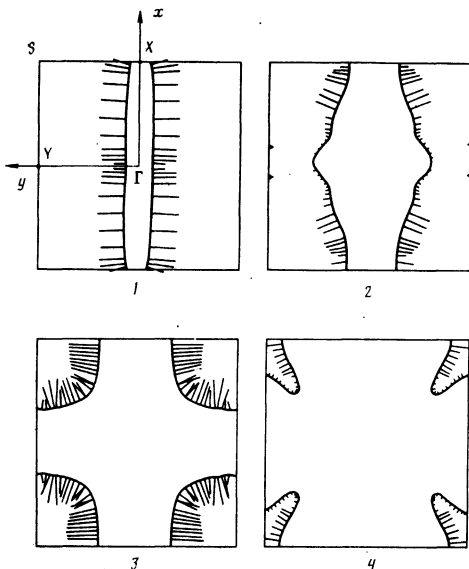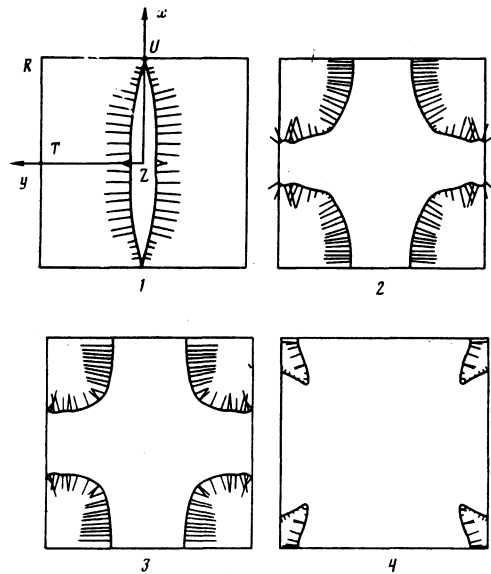
On the whole, the degree of corrugation of the Fermi surface of YBa$_2$Cu$_3$O$_7$ is higher than in the case of the Fermi surface of La$_2$CuO$_4$. Such a corrugation should favor stabilization of the crystal structure, which (together with a strong electron–phonon interaction[13]) can give rise to large values of T_c in the case of YBa$_2$Cu$_3$O$_{7-\delta}$.

We shall conclude by giving the values of a number of important numerical characteristics of the Fermi surface of YBa$_2$Cu$_3$O$_7$. These characteristics may be useful in developing a theory of high-temperature superconductivity. Important characteristics of the electron subsystem include the velocities of electrons on the Fermi surface. Figures 12 and 13 give the maps of velocities for two sections of the Fermi surface of YBa$_2$Cu$_3$O$_7$. It should be pointed out that the values of the velocities are almost constant in magnitude and direction on the electron cushion 1. The lowest velocities are observed for the fourth sheet of the Fermi surface. The strongest anisotropy of the electron velocity is observed for the second sheet, which exhibits the strongest corrugation. Table I gives the numerical values of the areas of the Fermi surface and the projections of the mean velocities, reciprocal velocities, the mean-square velocities of electrons, as well as the plasma frequencies. In contrast to Ref. 14, where similar results are given for all the Fermi surfaces, in the present case calculations were carried out for a much larger number of k points, so that we were able to determine these quantities separately for each sheet of the Fermi surface. The highest velocities are observed along the y direction for practically all the sheets of the Fermi surface and the lowest (as expect-

FIG. 12. Distribution of the velocities $V_k(E_F)$ in YBa$_2$Cu$_3$O$_7$ plotted for the $k_z = 0$ section.

TABLE I. Area of the whole Fermi surface and its separate sheets S, characteristic values of velocities averaged over the Fermi surface, and plasma frequencies $\omega_{p\alpha\alpha}$ for $YBa_2Cu_3O_7$.

Fermi surface sheet	$S \cdot 10^{16}$, cm^{-2}	Component α	$\langle v_\alpha \rangle \cdot 10^7$, cm/s	$\langle \frac{1}{v_\alpha} \rangle \cdot 10^{-7}$, s/cm	$[\langle v_\alpha^2 \rangle]^{1/2} \cdot 10^7$, cm/s	$\omega_{p\alpha\alpha}$, eV
1	3.596	x	0.37	7.61	0.48	0.41
		y	4.66	0.25	4.86	3.97
		z	0.56	8.71	0.82	0.66
2	5.139	x	1.02	12.51	1.52	1.71
		y	2.23	12.86	3.02	3.14
		z	0.53	10.67	0.92	1.05
3	4.055	x	2.38	2.03	2.90	2.72
		y	3.48	3.04	4.28	3.44
		z	0.32	16.91	0.49	0.43
4	3.137	x	0.63	7.09	0.74	1.05
		y	1.22	2.88	1.61	1.80
		z	0.18	30.29	0.29	0.41
$\sum_{i=1}^{4}$	15.915	x	1.14	7.29	1.75	3.40
		y	2.90	5.53	3.67	6.38
		z	0.42	14.88	0.71	1.38

ed) along the z direction. It should also be pointed out that in the case of an electron cushion the components of the velocities along the x direction are also very small. A very strong anisotropy is characteristic of plasma frequencies. Such an anisotropy of physical properties of $YBa_2Cu_3O_7$ is confirmed also by the experimental results. For example, direct measurements of the electrical resistivity tensor $\rho_{\alpha\beta}$ reported in Ref. 15 give $2\rho_{zz}/(\rho_{xx} + \rho_{yy}) \approx 30$, whereas according to the theoretical calculations reported in Ref. 14, this ratio is 10 and our estimates give ~ 9.5. In our opinion, an allowance for the strong anisotropy of the physical properties is important in developing a theory of high-temperature superconductivity.

The authors regard it as their pleasant duty to thank Prof. O. K. Andersen for discussing these results.

[1] J. G. Bednorz and K. A. Müller, Z. Phys. B **64**, 189 (1986).

[2] M. K. Wu, J. R. Ashburn, C. J. Torng, P. H. Hor, R. L. Meng, L. Gao, Z. J. Huang, Y. Q. Wang, and C. W. Chu, Phys. Rev. Lett. **58**, 908 (1987).

[3] S. Tanigawa, T. Kurihara, M. Osaws, et al., Proc. ICMT and MRS, Tokoyo, p. 1.

[4] L. Hoffmann, A. A. Manuel, M. Peter, and E. Walker, Proc. Intern. Conf. on High Temperature Superconductors and Materials and Mechanisms of Superconductivity, Interlaken, 1988, in: Physica C (Utrecht) **153-155**, Part 1, 129 (1988).

[5] C. S. Sundar, A. K. Sood, A. Bharathi, and Y. Hariharan, Proc. Intern. Conf. on High Temperature Superconductors and Materials and Mechanisms of Superconductivity, Interlaken, 1988, in: Physica C (Utrecht) **153-155**, Part 1, 155 (1988).

[6] A. Bharathi, Y. Hariharan, A. K. Sood, V. Sankara Sastry, et al., Proc. Intern. Conf. on High Temperature Superconductors and Materials and Mechanisms of Superconductivity, Interlaken, 1988, in: Physica C (Utrecht) **153-155**, Part 1, 111 (1988).

[7] J. Yu, A. J. Freeman, and J. H. Xu, Phys. Rev. Lett. **58**, 1035 (1987).

[8] L. F. Mattheiss and D. R. Hamann, Solid State Commun. **63**, 395 (1987).

[9] S. Massida, J. Yu, A. J. Freeman, and D. D. Koelling, Phys. Lett A **122**, 198 (1987).

[10] O. K. Andersen, Phys. Rev. B **12**, 3060 (1975).

[11] J. P. Perdew and A. Zunger, Phys. Rev. B **23**, 5048 (1981).

[12] V. V. Nemoshkalenko and V. N. Antonov, *Methods for Computation Physics in the Theory of Solids. Band Theory of Metals* [in Russian], Naukova Dumka, Kiev (1985).

[13] V. Bayot, F. Dellannay, C. Dewitte, J. P. Erauw, X. Gonze, J. P. Issi, A. Jonas, M. Kinany-Alaoui, M. Lambricht, J. P. Michenaud, J. P. Minet, and L. Piraux, Solid State Commun. **63**, 983 (1987).

[14] P. B. Allen, W. E. Pickett, and H. Krakauer, Phys. Rev. B **37**, 7482 (1988).

[15] S. W. Tozer, A. W. Kleinsasser, T. Penney, D. Kaiser, and F. Holtzberg, Phys. Rev. Lett. **59**, 1768 (1987).

Translated by A. Tybulewicz